

Scaling behavior of domain walls at the $T = 0$ ferromagnet to spin-glass transition

O. Melchert and A. K. Hartmann

Institut für Physik, Universität Oldenburg, 26111 Oldenburg, Germany

(Dated: November 3, 2018)

We study domain-wall excitations in two-dimensional random-bond Ising spin systems on a square lattice with side length L , subject to two different continuous disorder distributions. In both cases an adjustable parameter allows to tune the disorder so as to yield a transition from a spin-glass ordered ground state to a ferromagnetic groundstate. We formulate an auxiliary graph-theoretical problem in which domain walls are given by undirected shortest paths with possibly negative distances. Due to the details of the mapping, standard shortest-path algorithms cannot be applied. To solve such shortest-path problems we have to apply minimum-weight perfect-matching algorithms. We first locate the critical values of the disorder parameters, where the ferromagnet to spin-glass transition occurs for the two types of the disorder. For certain values of the disorder parameters close to the respective critical point, we investigate the system size dependence of the width of the the average domain-wall energy ($\sim L^\theta$) and the average domain-wall length ($\sim L^{d_f}$). Performing a finite-size scaling analysis for systems with a side length up to $L=512$, we find that both exponents remain constant in the spin-glass phase, i.e. $\theta \approx -0.28$ and $d_f \approx 1.275$. This is consistent with conformal field theory, where it seems to be possible to relate the exponents from the analysis of Stochastic Loewner evolutions (SLEs) via $d_f - 1 = 3/[4(3+\theta)]$. Finally, we characterize the transition in terms of ferromagnetic clusters of spins that form, as one proceeds from spin-glass ordered to ferromagnetic ground states.

PACS numbers: 75.50.Lk, 02.60.Pn, 75.40.Mg, 75.10.Nr

Keywords:

I. INTRODUCTION

Ising spin glasses (ISGs) are among the most-basic models of disordered systems that allow for the study of phase transitions in the presence of quenched disorder. ISGs are elaborately studied in statistical physics [1, 2, 3, 4] and despite several decades of active research they attract a constant interest, challenging with still not well understood traits and unresolved questions. In the scope of this paper we investigate ground state (GS) spin configurations and minimum-energy domain-wall (MEDW) excitations in a $2d$ random-bond ISG. In brief, MEDWs are topological excitations that are induced by a change of the boundary conditions (BCs) from periodic to antiperiodic along one boundary of the system. In particular we are interested in the scaling properties of MEDWs close to the critical point at which the $T=0$ spin glass (SG) to ferromagnet (FM) transition occurs. From a phenomenological point of view, the physics of the SG ordered phase of ISGs with short ranged interactions, like the $2d$ model considered here, can be described in terms of the droplet scaling picture [5, 6, 7]. Therein, the low-temperature behavior is dominated by droplet excitations, i.e. clusters of spins that are flipped relative to the GS spin configuration. Within the droplet picture, excitations like MEDWs posses an excitation energy ΔE that scales with system size L as $\Delta E \sim L^\theta$, where θ is referred to as stiffness exponent. The value of θ is assumed to be universal for all types of excitations and constant within the whole SG phase. Moreover, in a statistical sense, they are self-similar fractals characterized by a fractal dimension d_f that is defined by the scaling of the average MEDW length as $\langle l \rangle \sim L^{d_f}$. The advan-

tage of working at zero temperature is that the GS problem for the particular setup studied here can be solved by means of exact combinatorial-optimization algorithms [8, 9, 10, 11, 12] whose running time increases only polynomially with the system size. Hence, very large systems can be treated exactly, giving very precise and reliable estimates for the observables. For $2d$ lattices, where the interaction strengths (bonds) between adjacent spins are drawn from a Gaussian distribution with zero mean and unit width, domain wall (DW) calculations using such algorithms resulted in the estimates $\theta = -0.287(4)$ [13, 14] and $d_f = 1.274(2)$ [15]. The negative value of the stiffness exponent indicates that the excitation energy required to introduce a MEDW gets negligibly small as $L \rightarrow \infty$ and thus, thermal fluctuations prevent a spin-glass ordering for any non-zero temperature. The above value of the stiffness exponent was later on confirmed for continuous disorder distributions different from the Gaussian bond distribution [16], for droplet excitations respecting a Gaussian distribution of the bonds [17, 18, 19] and quite recently also for droplets within the $\pm J$ model [20]. Furthermore, recent studies suggested that MEDWs respecting a Gaussian distribution of the bonds can be described by stochastic Loewner evolutions (SLEs) [21, 22]. SLEs are generated by a stochastic differential equation driven by a brownian motion. They describe the continuum limit for various $2d$ random curves and their geometric properties relate to the statistics of several critical interfaces [23]. Within conformal field theory it further seems to be possible to relate the DW fractal dimension to the stiffness exponent by means of the relation $d_f - 1 = 3/[4(3+\theta)]$, subsequently referred to as SLE scaling relation. For the pure spin glass, this is in agreement

with the numerical estimates of θ and d_f stated above.

Here, we consider a random-bond Ising model that allows us to investigate the SG to FM transition at zero temperature, by tuning the mean value of the underlying disorder distribution. In a previous work, the related $\pm J$ model was studied in $2d$ [16]. There exact matching algorithms to find ground states (GSs) were applied. It was found that, in the limit of large system sizes, the SG to FM transition occurs at a fraction $p_c = 0.103(1)$ of antiferromagnetic bonds ($-J$) among ferromagnetic bonds ($+J$). Further, the critical exponents ν and β that describe the divergence of the correlation length and the order parameter, were found to be $\nu = 1.55(1)$ and $\beta = 0.09(1)$. Due to the discreteness of the distribution, the DWs are not unique and cannot be sampled in equilibrium for large systems. Hence the fractal dimension has not been determined in a precise way so far.

To clarify whether the SLE scaling relation above holds within the whole spin-glass phase, we use two different continuous distributions of the disorder, which allow us to calculate the fractal dimension d_f with high precision. For this purpose, we perform GS calculations by means of exact combinatorial-optimization algorithms and study the scaling behavior of MEDWs close to the critical point where the SG to FM transition occurs. At first, we perform a finite-size scaling analysis for systems of moderate sizes ($L \leq 64$) to locate the critical points at which the transitions takes place. Then we perform additional simulations for large systems ($L \leq 512$) close to and directly at the critical points, to get a grip on the scaling behavior of the MEDWs. Finally, we characterize the transition using a finite-size scaling analysis for the largest and second-largest ferromagnetic clusters of spins within the GS spin configurations. These clusters form as one proceeds from spin-glass ordered to ferromagnetic ground states. To summarize our results: we find that the SLE scaling relation holds in the SG phase up to a point very close to the respective critical points, but not right at the critical points. Moreover, MEDWs in the SG phase scale like self-similar fractals, while MEDWs in the ferromagnetic phase display a self-affine scaling behavior.

The paper is organized as follows. In section II we introduce the model and describe the algorithmic techniques we have used in order to obtain MEDWs. In section III we present the results of our numerical simulations. We conclude with a summary in section IV.

II. MODEL AND METHOD

We performed GS calculations for two-dimensional random-bond Ising spin systems with nearest-neighbor interactions. The respective model consists of $N = L \times L$ spins $\sigma = (\sigma_1, \dots, \sigma_N)$ with $\sigma_i = \pm 1$, located on the sites of a regular square lattice. The energy of a given spin configuration is measured by the Edwards-Anderson

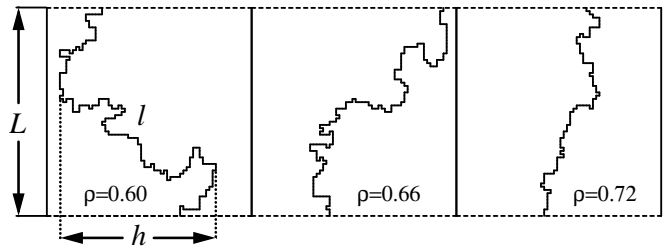


FIG. 1: Domain wall samples for systems of side-length $L = 64$ and different values of the disorder parameter ρ (Model I). The samples are taken in the SG phase ($\rho = 0.60$), right at the critical point ($\rho = 0.66$) and in the FM phase ($\rho = 0.72$). Besides the system size L , the DW length l and its roughness h are illustrated.

Hamiltonian

$$H(\sigma) = - \sum_{\langle i,j \rangle} J_{ij} \sigma_i \sigma_j, \quad (1)$$

where the sum runs over all pairs of adjacent spins with periodic BCs in the x -direction and free BCs in the y -direction. Therein, the bonds J_{ij} are quenched random variables drawn from a given disorder distribution. Subsequently, we distinguish two types of the bond disorder:

(1) Model I, where one realization of the disorder consists of a random fraction ρ of ferromagnetic bonds and a fraction $(1 - \rho)$ of bonds that are drawn from a Gaussian distribution with zero mean and unit variance, i.e.

$$P_I(J) = (1 - \rho) \exp(-J^2/2)/\sqrt{2\pi} + \rho \delta(J - 1). \quad (2)$$

There exists a critical value ρ_c of the disorder parameter that separates a spin-glass phase ($\rho < \rho_c$) from a ferromagnetic phase ($\rho > \rho_c$). As limiting cases we can identify the pure Ising SG at $\rho = 0$ and the ordinary Ising ferromagnet at $\rho = 1$. A similar type of disorder was used earlier for Monte Carlo simulations that were carried out to study the FM to SG transition in $3d$ and to numerically verify the absence of an equilibrium “mixed” ferromagnetic-SG phase for the respective model [24].

(2) Model II, where the bond strengths are drawn from a Gaussian distribution with mean μ_J and width σ_J , i.e.

$$P_{II}(J) = \exp(-(J + \mu_J)^2/(2\sigma_J^2))/(\sqrt{2\pi}\sigma_J). \quad (3)$$

As a function of the reduced variable $r = \sigma_J/\mu_J$ we expect to find a ferromagnetic phase (spin-glass phase) for $r < r_c$ ($r > r_c$). An earlier DW renormalization-group study of small systems [25] supported by transfer-matrix calculations reported, amongst other things, a zero temperature FM to SG transition at $r_c = 0.961(10)$ with $\nu = 1.42(8)$. Further, for the pure SG ($\mu_J = 0$), an extrapolation of the DW free energy to zero temperature resulted in a stiffness exponent $\theta = -0.281(5)$. The fractal properties of the DWs were not studied in this work.

In the above two models, the bonds are allowed to take either sign, where a value $J_{ij} > 0$ signifies a ferromagnetic

coupling that prefers a parallel alignment of the coupled spins, while a value $J_{ij} < 0$ indicates an antiferromagnetic coupling in favor of antiparallel aligned spins. The competing nature of these interactions gives rise to frustration. A plaquette, i.e. an elementary square on the lattice, is said to be frustrated if it is bordered by an odd number of antiferromagnetic bonds. In effect, frustration rules out a GS in which all the bonds are satisfied.

Here, our intention is to get a grip on the geometric properties of minimum-energy DWs. These are topological excitations that are defined, for each realization of the bond disorder, relative to two spin configurations: σ_p , a GS spin configuration with respect to periodic BCs further characterized by the configurational energy E_p and σ_{ap} , a GS respecting antiperiodic BCs characterized by the energy E_{ap} . Antiperiodic BCs are realized by inverting the sign of all the bonds along one column in the x -direction. Comparing the orientation of the spins in the two GSs, one can distinguish two regions on the lattice: one where the orientation of a spin is the same in both GSs and another, where the orientation of a spin differs regarding the two GSs. Within these regions, the bonds between adjacent spins are either satisfied or broken in both GSs likewise. Bonds that connect spins that belong to different regions on the lattice are satisfied in exactly one of the two GSs. The MEDW is the interface in between the two regions and as such, it runs perpendicular to the latter bonds. It has the property that its excitation energy $\delta E = E_{ap} - E_a$ is minimal among all possible DWs that span the system in the direction with the free BCs. The basic observables related to a DW are its over all length l , its roughness h and its excitation energy δE . MEDWs for three different values of the disorder parameter ρ introduced above (see Model I) are illustrated in figure 1.

We now give a brief description of the algorithm that we used to determine the MEDWs. A more extensive description of the individual steps of the algorithm can be found in [15]. For a given realization of the bond disorder, we first determine a GS spin configuration consistent with periodic BCs in the x -direction. Besides the magnetization $m_L = |\sum_i \sigma_i|/L^2$ and the energy, this tells which bonds are satisfied/broken in the GS for that particular disorder sample. For the $2d$ ISG on planar lattice graphs, i.e. when there are periodic BCs in at most one direction, exact GS spin configurations can be found in polynomial time. This is possible through a mapping to an appropriate minimum-weight perfect-matching problem [8, 9, 10], a combinatorial-optimization problem known from computer science. Here, we state only the general idea of this method. For this mapping, the spin system needs to be represented by its frustrated plaquettes and paths connecting those pairwise, i.e. *matching* them. In doing so, individual path segments are confined to run perpendicular across bonds on the spin lattice. Those bonds that are crossed by path segments are not satisfied in the corresponding spin configuration. The *weight* of the matching is just the sum of the absolute values of all bond

strengths that relate to unsatisfied bonds. Hence, finding a minimum-weight perfect matching on the graph of frustrated plaquettes then corresponds to finding a spin configuration with a minimal configurational energy, hence a GS. The use of this approach permits the treatment of large systems, easily up to $L = 512$, on single processor systems. This GS spin configuration can further be used to set up a weighted dual of the spin lattice, whose weighted edges comprise all possible DW segments. The weighted dual is constructed as follows: set up a new graph $G = (V, E, \omega)$, whose sites $i \in V$ relate to the elementary plaquettes on the spin lattice. Its necessary to introduce two *extra* sites that account for the free BCs. Two sites are joined by an undirected edge $e \in E$, if the corresponding plaquettes have a bond in common. For the weight assignment on the dual, consider a bond on the spin lattice having a coupling strength J_{ij} . If the bond is satisfied (broken) regarding the GS, the corresponding dual edge e gets a weight $\omega(e) = -2|J_{ij}|$ ($\omega(e) = +2|J_{ij}|$). The weighted dual now comprises all possible DW segments, where the weight of an edge is equal to the amount of energy that it would contribute to a DW. Every possible DW links both extra sites on the dual, where the energy of a DW is the sum of the weights along the according lattice path. So as to have minimum energy, it is beneficial for a DW to include (avoid) edges with a negative (positive) edgeweight. Consequently, a MEDW is a minimum-weight path on the dual that joins both extra sites. The dual G is an undirected graph that allows for negative edge weights and so as to construct minimum-weight paths on G , it requires matching techniques [26]. Therefore we need to map the dual to an auxiliary graph G_A and find a minimum-weight perfect matching on G_A which we finally can relate to a minimum-weight path on G . For each realization of the disorder, this procedure yields an explicit representation of the minimum-energy DW that we can easily probe for its geometric properties. A more detailed description of the algorithm can be found in [15]. In the following we will use the procedure outlined above to investigate MEDWs for the random-bond Ising models introduced earlier.

III. RESULTS

So as to characterize the scaling behavior of MEDWs for the two disorder distributions introduced above, we first of all need to find the critical values ρ_c (Model I) and r_c (Model II) of the disorder parameters at which the $T=0$ SG to FM transition takes place. Reliable estimates for the location of the critical points can already be obtained from comparatively small system sizes, here we use $L = 24, 32, 48, 64$. In general, one has to find a proper balance of system size and sample numbers that affect finite-size effects and statistical error, respectively [27]. Subsequently we can probe the asymptotic scaling behavior of the MEDWs at fixed values of the disorder

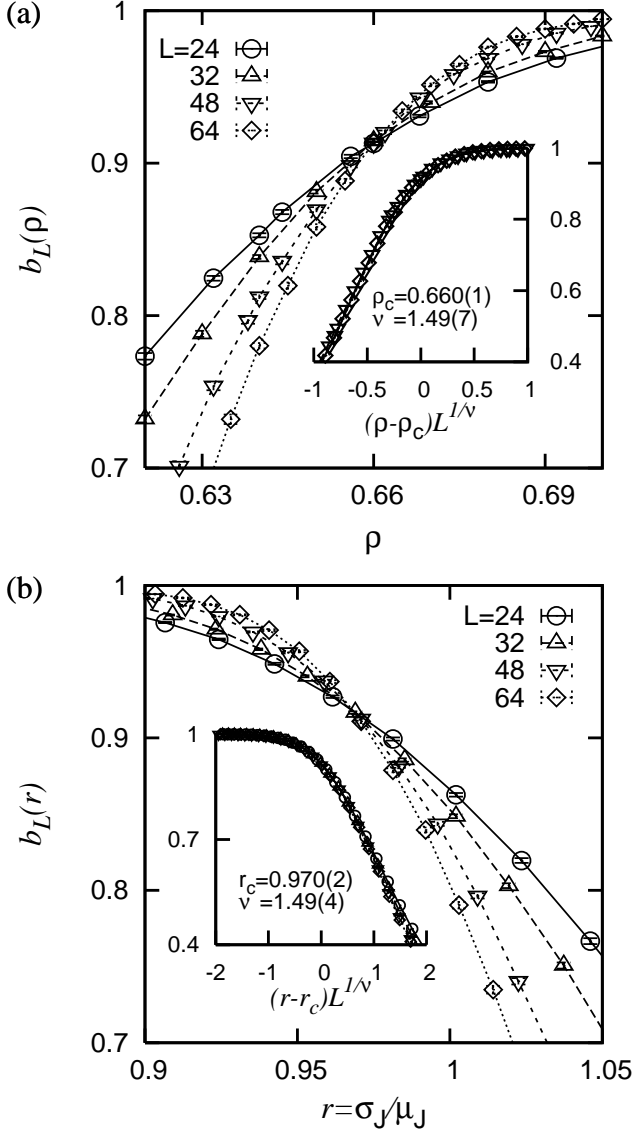


FIG. 2: Results of the FSS analysis for the Binder parameter b_L associated with the magnetization, for different system sizes L . The main plot shows the unscaled data near the critical point, while the inset illustrates the data collapse obtained for (a) Model I: $\rho_c = 0.660(1)$ and $\nu = 1.49(7)$, (b) Model II: $r_c = 0.970(2)$ and $\nu = 1.49(4)$.

parameters close to the critical points for large system sizes up to $L=512$.

A. Finite-size scaling analysis to characterize the $T=0$ spin glass to ferromagnet transition

First, we will discuss the results for the Model I disorder and afterwards report the results for the Model II disorder more briefly. As pointed out above, at large values of ρ , there exists an ordered ferromagnetic phase, while for small values of ρ a spin-glass phase exists. Therefore,

a proper order parameter to characterize the respective SG-FM transition is the magnetization $m_L = |\sum_i \sigma_i|/L^2$ for a system of size L . In the following, we perform a finite-size scaling analysis (FSS) in order to locate the critical point ρ_c and also estimate the critical exponents that describe the scaling behavior of the magnetization at criticality. The Binder parameter [28] associated with the magnetization reads

$$b_L = \frac{1}{2} \left(3 - \frac{\langle m_L^4 \rangle}{\langle m_L^2 \rangle^2} \right) \quad (4)$$

and is expected to scale as $b_L(\rho) \sim f_1[(\rho - \rho_c)L^{1/\nu}]$, where f_1 is a size-independent function and ν signifies the critical exponent that describes the divergence of the correlation length as the critical point is approached. Here, we simulated square systems of size $L = 24, 32, 48, 64$ at various values of the disorder parameter ρ . Observables are averaged over up to 3×10^4 (2×10^4) samples for the smallest (largest) systems and we utilized the data collapse anticipated by the scaling assumption above to obtain $\rho_c = 0.660(1)$ and $\nu = 1.49(7)$ with a quality $S = 1.25$ of the data collapse [29], see figure 2(a). The value of the critical exponent ν agrees within errorbars with the value $\nu = 1.42(8)$ obtained using a transfer-matrix approach [25]. Note that both, the numerical values of ρ_c and ν further agree with those that characterize the negative-weight percolation of loops and paths on 2d lattices [30], highlighting the close connection of the two optimization problems. The order parameter of the transition is expected to scale conform with the assumption $m_L(\rho) \sim L^{-\beta/\nu} f_2[(\rho - \rho_c)L^{1/\nu}]$, f_2 being a size-independent function, where the magnetization exponent β was obtained after fixing ν and ρ_c to the values stated above. The most satisfactory data collapse ($S = 1.83$) was obtained using $\beta = 0.097(6)$, see figure 3. In general, the above scaling relation holds best near the critical point and one can expect that there are corrections to scaling off criticality. As a remedy, we restricted the latter scaling analysis to the interval $[-0.5, +0.2]$, enclosing the critical point on the rescaled abscissa. Note that the values for the exponents found here agree with those found from GS calculation for the $\pm J$ -model [31] within the errorbars. As an alternative order parameter, we also studied the average path length $\langle l \rangle$ of the MEDWs, where we expect a scaling of the form

$$\langle l \rangle \sim L^{d_f^c} f_3[(\rho - \rho_c)L^{1/\nu}]. \quad (5)$$

Therein, d_f^c signifies the fractal dimension of the DWs at the critical point and f_3 is another size-independent function. From a finite-size scaling analysis restricted to the interval $[-0.75, +0.5]$ on the rescaled abscissa, we obtained $d_f^c = 1.222(4)$ with a quality $S = 1.33$, see figure 4 (Note that for a more clear presentation, the argument along the abscissa in figure 4 reads $|\rho - \rho_c|L^{1/\nu}$). For the somewhat larger interval $[-1, +0.5]$ we found $d_f^c = 1.223(4)$ with $S = 1.40$ in agreement with the above value. Since we expect the average MEDW length at $\rho = 0$ to

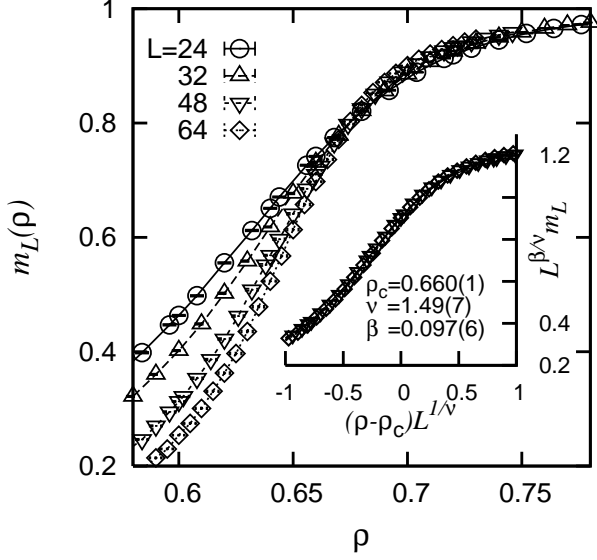


FIG. 3: Results of the FSS for the average magnetization $m_L(\rho)$ for different system sizes L for Model I disorder. The main plot shows the unscaled data near the critical point, while the inset illustrates the data collapse obtained for the parameters $\rho_c = 0.660(1)$, $\nu = 1.49(7)$ and $\beta = 0.097(6)$.

scale as $\langle l \rangle \sim L^{d_f}$ (here, $\rho = 0$ corresponds to the pure spin glass studied in [15]), where $d_f = 1.274(2)$, we can further estimate the asymptotic behavior $f_3(x) \sim x^{\nu(d_f - d_f^c)}$ of the scaling function in Eq. (5) as $x \rightarrow -\infty$. This can be seen from the top branch in figure 4, where the function $f_3(x) \sim x^{0.08(1)}$ is shown as solid line and agrees well with the data. Note that via Eq. (5) the DWs at ρ_c exhibit the fractal dimension d_f^c , while for all values $\rho < \rho_c$, the fractal dimension is given by d_f . Hence, the scaling ansatz Eq. (5) is based on the assumption that behavior in the SG phase is universal, which is tested below for much larger systems explicitly.

For the “ferromagnetic” branch ($x \rightarrow +\infty$), a similar consideration yields the asymptotic scaling $f_3(x) \sim x^{-0.33(1)}$, indicated as a dashed line in figure 4.

Further, we found that the probability $P_L(\rho)$ that the MEDW roughness is equal to L scales as $P_L(\rho) = f_4[(\rho - \rho_c)L^{1/\nu}]$, shown in the inset of figure 4. In the ferromagnetic phase the value of P_L tends towards zero and in the spin-glass phase it saturates around $P_L \approx 0.12$. Hence, as pointed out in [24], an asymptotic nonzero probability that the MEDW roughness is $O(L)$ can be used as an order parameter to detect the SG phase.

Regarding Model II, we simulated systems of size $L = 24, 32, 48, 64$ at different values of the disorder parameter r . Here, we fixed the width of the disorder distribution to the value $\sigma_J = 1$ and we vary only its mean μ_J . Observables are averaged over up to 3×10^4 (2×10^4) samples for the smallest (largest) systems and we utilized the data collapse anticipated by the scaling assumptions for the Binder parameter (see figure 2(b)) and the magnetization (not shown) to obtain the values $r_c = 0.970(2)$,

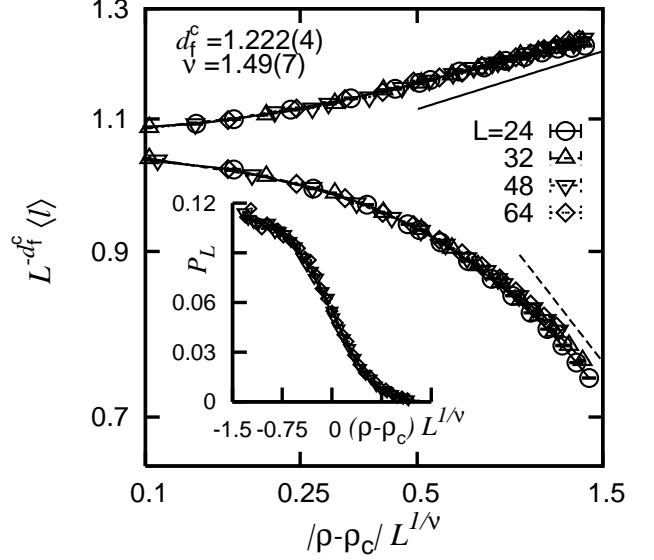


FIG. 4: Results of the FSS analysis for Model I disorder. The main plot illustrates the FSS of the average MEDW length $\langle l \rangle$ for different system sizes L , where the best data collapse is obtained for the parameters $\rho_c = 0.660(1)$, $\nu = 1.49(7)$ and $d_f^c = 1.222(4)$. The solid and dashed lines illustrate the asymptotic scaling behavior of both branches as described in the text. The inset shows the scaling of the probability $P_L(\rho)$ that the roughness of the MEDW is equal to the system size L .

$\nu = 1.49(4)$ ($S = 1.0$) and $\beta = 0.09(1)$ ($S = 0.46$). Note that the numerical values of r_c and ν agree within errorbars with the values $r_c = 0.961(10)$ and $\nu = 1.42(8)$ obtained using a transfer-matrix approach [25]. The scaling of the average MEDW length here yields a numerical value $d_f = 1.249(5)$ ($S = 1.99$) which can only be considered as an effect of the finite system size, see the discussion below. Further, the probability that the MEDW roughness equals L tends towards $P_L \approx 0.12$ in the SG phase, in agreement with the above results.

B. Scaling behavior at fixed values of ρ and r

We have carried out further simulations at a couple of selected values of ρ and r , see tables I and II, in order to probe the asymptotic scaling behavior of MEDWs regarding the two disorder distributions introduced above. We therefore considered systems of size up to $L = 512$ with 10^3 realizations of the disorder. In particular, we are interested in the asymptotic scaling behavior of the average MEDW length $\langle l \rangle$ with respect to the system size L , defining the DW fractal dimension d_f via $\langle l \rangle \sim L^{d_f}$. We further study the scaling of the average MEDW roughness $\langle h \rangle$, i.e. the extension of the lattice path in the direction of the periodic BCs, that defines the roughness exponent d_r by means of $\langle h \rangle \sim L^{d_r}$. Both these observables relate only to the geometric properties of the MEDW, see figure 1. Finally, we investigate the

size scaling of the mean $\Delta E = \langle |\delta E| \rangle \sim L^{\theta_1}$ and width $\sigma(\delta E) = \sqrt{\langle \delta E^2 \rangle - \langle \delta E \rangle^2} \sim L^{\theta_2}$ of the distribution of MEDW excitation energies.

Again, we first discuss the results for the Model I disorder and afterwards state the results for the Model II disorder more briefly. The asymptotic scaling behavior of the average DW length allows one to obtain the fractal dimension by using a direct fit to the power law data over the entire range of system sizes L . A reliable and more systematic alternative is to investigate a sequence of effective (local) exponents $d_f^{\text{eff}}(L)$ that describe the scaling of $\langle l \rangle$ within intervals of, say, 3 successive values of L . The change of the effective exponents for increasing system sizes further show how the scaling behavior is affected by the finite size of the simulated systems. From the sequence of effective exponents one can extrapolate the asymptotic fractal dimension by means of a straight line fit to the plot of $d_f^{\text{eff}}(L)$ against the inverse system size $1/L$. Figure 5 shows the effective exponents obtained for 3 and 4 successive values of L at different values of the disorder parameter ρ . Therein, the asymptotic fractal dimensions d_f , as listed in table I, where estimated from the effective exponents resulting from intervals of 4 successive system sizes. The asymptotic values for d_r , θ_1 and θ_2 , listed in tables I/II, where estimated using a similar procedure. Our results for the fractal dimension and the stiffness exponent at $\rho = 0.60$ and 0.62 clearly support the estimates for the pure SG at $\rho = 0$. They are in agreement with the SLE scaling relation and hence we could verify that the SLE scaling relation holds up to values of the disorder parameter close to ρ_c .

At the critical point we find that the estimates of d_f and θ_2 are not in agreement with the SLE scaling relation. However, MEDWs at ρ_c are self-similar with the scaling dimension $d_f = 1.222(1)$ and a roughness compatible with unity. Here, the numerical value of d_f as estimated from the effective exponents compares nicely to the value $d_f = 1.222(4)$ found from the previous FSS.

We further find that d_f and θ_2 in the ferromagnetic phase above the critical point are not consistent with the SLE scaling relation. There, the overall length of the DW increases linear with the system size, i.e. the

ρ	d_f	d_r	θ_1	θ_2
0.00	1.274(2)	1.008(11)	-0.287(4)	-0.287(4)
0.60	1.275(1)	1.003(3)	-0.28(1)	-0.28(2)
0.64	1.275(2)	1.012(4)	-0.28(1)	-0.28(4)
0.66	1.222(1)	1.002(2)	0.17(2)	0.16(1)
0.68	1.05(2)	0.74(3)	0.97(4)	0.35(3)
0.72	1.022(1)	0.698(6)	1.052(3)	0.27(2)

TABLE I: From left to right: disorder parameter, fractal dimension, roughness exponent and exponents that describe the scaling of the mean and width of the MEDW energy distribution. The figures for $\rho = 0$ are taken from [15].

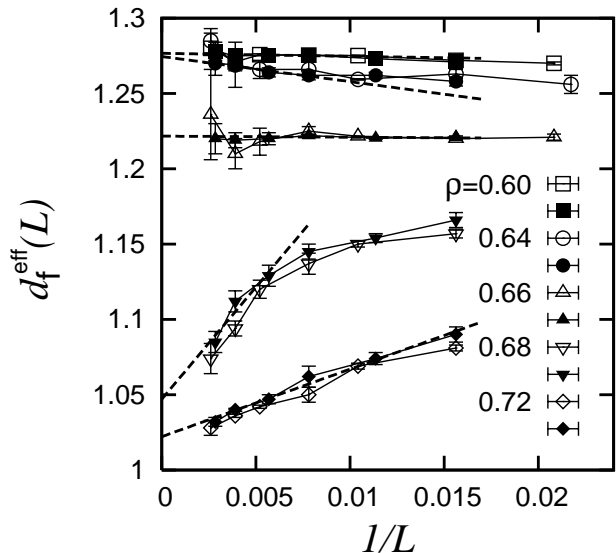


FIG. 5: Extrapolation of the asymptotic fractal dimension for Model I. Analysis of the sequence of effective exponents $d_f^{\text{eff}}(L)$ that describe the scaling of the average MEDW length within intervals of 3 (open symbols) and 4 (filled symbols) successive values of L , according to $\langle l \rangle \sim L^{d_f}$. The asymptotic value of the fractal dimension d_f is extrapolated from the plot of d_f^{eff} against $1/L$ as the intersection of a straight line fit to the data with the ordinate.

fractal dimension extrapolates towards $d_f = 1$, whereas for the roughness exponent $d_r < 1$ is found. This indicates that, albeit the MEDW is allowed to bend and turn back and forth on the lattice, the resulting overhangs are not significant for their scaling behavior. Further, the cost needed to introduce the DW grows almost linearly with the system size, while the rms-fluctuation is characterized by an exponent significantly smaller than that. Hence, MEDWs in the ferromagnetic phase display a self-affine scaling, governed by exponents that are in reasonable agreement with those that describe the scaling of the transverse deviation ($\sim L^{2/3}$) and the rms excitation energy ($\sim L^{1/3}$) of pinned DWs in an ordinary

r	d_f	d_r	θ_1	θ_2
∞	1.274(2)	1.008(11)	-0.287(4)	-0.287(4)
1.111	1.275(7)	0.994(4)	-0.294(6)	-0.295(5)
1.010	1.286(3)	1.024(2)	-0.311(2)	-0.35(1)
0.970	1.222(6)	0.999(3)	0.15(1)	0.15(1)
0.935	1.085(4)	0.782(3)	0.96(2)	0.31(2)
0.833	1.015(1)	0.651(3)	1.028(1)	0.31(2)

TABLE II: From left to right: disorder parameter $r = \sigma_J/\mu_J$, fractal dimension, roughness exponent and exponents that describe the scaling of the mean and width of the MEDW energy distribution. The figures for $r = \infty$, i.e. $\mu_J = 0$, are taken from [15].

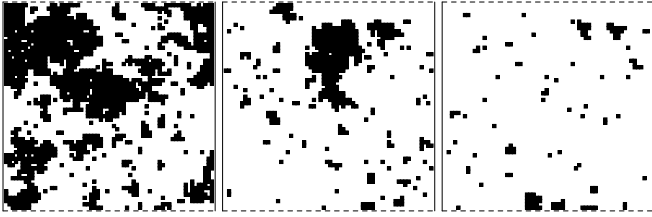


FIG. 6: Samples of GS spin configurations for systems of side-length $L = 64$ and $r = 1.1, 0.969, 0.9$ (from left to right) for Model II.

Ising FM with randomly placed impurities [32]. Further, the scaling behavior found here agrees with that observed for directed and undirected optimal paths on $2d$ lattices subject to weak disorder [33] or analogously the scaling of directed polymers in random media [34].

For the Model II disorder, our findings are qualitatively the same, hence we only state the numerical results without showing figures. The numerical values of d_f and θ_2 within the SG phase ($r > r_c$) are in agreement with the SLE scaling relation proposed for the pure SG. In particular, at $r = 1.01$ we find $d_f = 1.286(3)$ and $\theta_2 = -0.35(1)$. Here, the data for $\langle l \rangle$ gives a nice straight line on a double logarithmic scale, where we find $d_f = 1.284(2)$ from a fit to the pure power law data excluding $L \leq 100$. The situation for the data corresponding to $\sigma(\delta E)$ is somewhat different, i.e. the data still exhibits a curvature within the range of accessible system sizes on a double logarithmic scale. This does not allow to fit all the data at once, assuming a power law fit-function. Consequently, the most reliable estimate of the asymptotic value of θ_2 can be obtained by an analysis of the local exponents as described above. The reason for this difficulty might stem from the fact that the value $r = 1.01$ of the disorder parameter is located in the transition region close to the critical point. Albeit these values differ slightly from the values $\theta_2 \approx -0.28$ and $d_f \approx 1.274$ that one would expect to find in the SG phase, they are in agreement with the SLE scaling relation. The numerical values for the exponents right at the critical point are again not in agreement with the proposed scaling relation. However, the asymptotic fractal dimension extrapolated from the effective exponents reads $d_f = 1.222(6)$ and is in agreement with the corresponding value at the critical point for the Model I disorder. Further, if we analyze the scaling of the average MEDW length restricted to system sizes $L < 64$ we find a value of $d_f = 1.246(4)$, consistent with the value encountered in the previous FSS analysis that was denoted as a finite-size effect. Within the ferromagnetic phase ($r < r_c$), MEDWs again display a self-affine scaling behavior, further characterized by exponents that extrapolate towards those that describe the scaling of the transverse deviation and the rms excitation energy of pinned DWs in an ordinary Ising FM with randomly placed impurities.

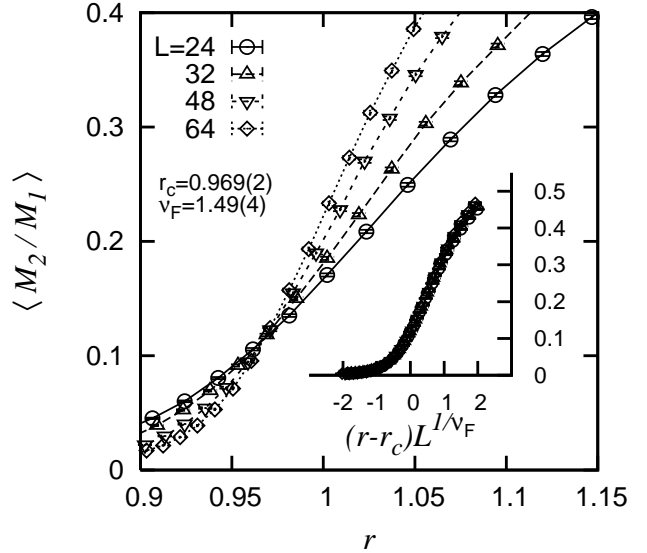


FIG. 7: FSS analysis of ferromagnetic domains at $T = 0$ for Model II. The main plot shows the average size-ratio $\langle M_2/M_1 \rangle$ of the second-largest and largest ferromagnetic clusters and the inset illustrates the data collapse under the respective scaling assumption, obtained for $r_c = 0.969(2)$ and $\nu_F = 1.49(4)$.

C. Finite-size scaling analysis of ferromagnetic spin domains at the $T=0$ spin glass to ferromagnet transition

As we decrease the value of the disorder parameter in Model II from $r = \infty$ (SG-phase) to $r < r_c$ (FM-phase), we can identify ferromagnetic clusters of spins, i.e. groups of nearest-neighbor spins with similar orientation, with increasing size (see Fig. 6). Here, as an alternative way to characterize the SG to FM transition at $T=0$, we perform a FSS analysis of the largest and second largest ferromagnetic clusters found for the GS spin configuration for each realization of the disorder. Such an analysis has been performed previously for standard percolation [35]. As above, we simulated systems of size $L = 24, 32, 48, 64$ at different values of the disorder parameter r . We kept the width of the disorder distribution at the fixed value $\sigma_J = 1$ and we vary only its mean μ_J . Observables are averaged over 2×10^4 samples for each system size. Subsequently, the relative size of a cluster specifies the number of spins that comprise the cluster divided by the number of spins on the lattice. Within our analysis we found that the average ratio $\langle M_2/M_1 \rangle$ of the relative sizes of the second-largest and the largest ferromagnetic clusters scales as

$$\langle M_2/M_1 \rangle \sim f_5[(r - r_c)L^{1/\nu_F}], \quad (6)$$

therein r_c is the location of the critical point and ν_F signifies the correlation length exponent. From a data collapse, restricted to the interval $[-1.5, +1.5]$ on the rescaled abscissa, we obtain the numerical values $r_c =$

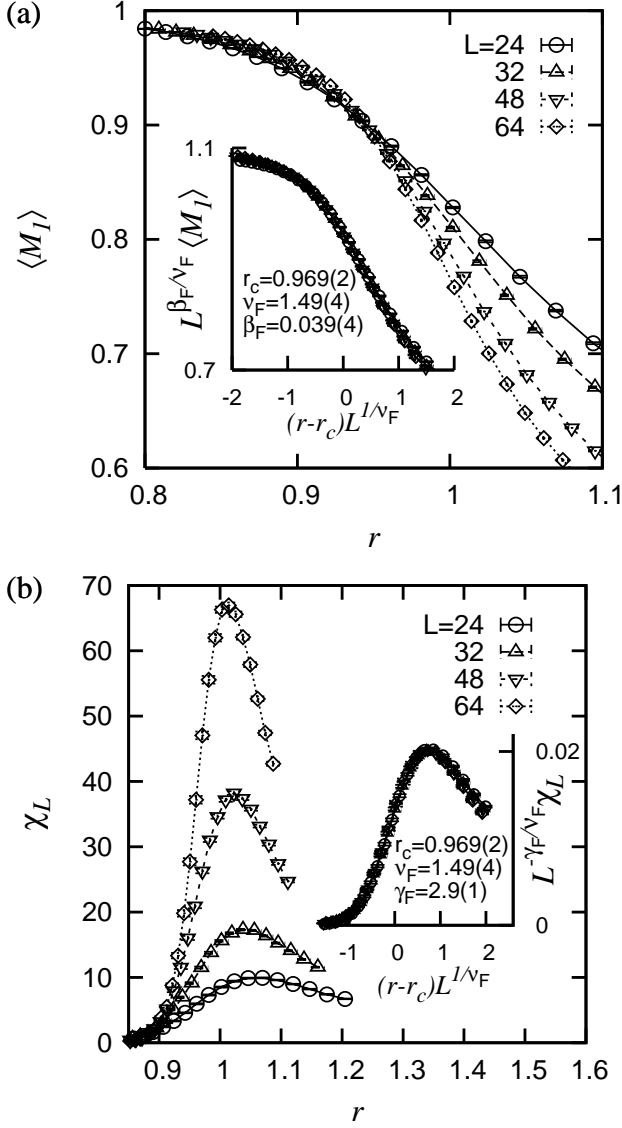


FIG. 8: FSS analysis of ferromagnetic domains at $T = 0$ for Model II. (a) normalized size $\langle M_1 \rangle$ of the largest ferromagnetic cluster, and (b) finite-size susceptibility $\chi_L = N[\langle M_1^2 \rangle - \langle M_1 \rangle^2]$ associated with the size of the largest cluster. The main plots show the unscaled data near the critical point, while the insets illustrate the data collapse under the respective scaling assumptions.

0.969(2) and $\nu_F = 1.49(4)$ with a quality $S = 0.85$, see figure 7. Both values agree within errorbars with those obtained from the Binder parameter analysis. If we allow for a nonzero scaling dimension according to $\langle M_2/M_1 \rangle \sim L^{-\kappa} f_6[(r-r_c)L^{1/\nu_F}]$, we yield r_c and ν_F as above and further $\kappa = 0.004(13)$ ($S = 0.82$, $[-2.0, +1.0]$). The numerical value of κ is compatible with zero and hence supports the scaling assumption (6) for the size ratio. Moreover, right at r_c we found the critical value $\langle M_2/M_1 \rangle = 0.122(1)$. For completeness we note, that we yield qualitatively similar findings for the ratio $\langle M_2 \rangle / \langle M_1 \rangle$ with

the critical value $\langle M_2 \rangle / \langle M_1 \rangle = 0.098(1)$. The difference between the two ratios is simply due to the cluster-size fluctuations at criticality.

As an order parameter we measure the relative size M_1 of the largest ferromagnetic cluster for each of the GSs. From the scaling assumption $\langle M_1 \rangle \sim L^{-\beta_F/\nu_F} f_7[(r-r_c)L^{1/\nu_F}]$ and the values of r_c and ν_F stated above we obtain $\beta_F = 0.039(4)$ ($S = 0.54$, $[-0.5, +0.5]$), see figure 8(a). A similar scaling assumption for the second largest cluster yields $\beta_{F,2} = 0.05(3)$ ($S = 0.26$, $[-0.5, +0.25]$, not shown). Albeit the numerical value of $\beta_{F,2}$ is less precise and somewhat larger compared to β_F , both exponents are compatible with Eq. (6).

The finite-size susceptibility $\chi_L = N[\langle M_1^2 \rangle - \langle M_1 \rangle^2]$ describing the fluctuations of the size of the largest ferromagnetic cluster, obeys the scaling form $\chi_L \sim L^{\gamma_F/\nu_F} f_8[(r-r_c)L^{1/\nu_F}]$ with another critical exponent γ_F , see figure 8(b). Together with the values of r_c and ν_F we estimate $\gamma_F = 2.9(1)$ ($S = 0.85$, $[-1.5, +1.0]$). These exponents further are in agreement with the hyperscaling relation $\gamma_F/\nu_F + 2\beta_F/\nu_F = d$.

We performed further simulations for the $\pm J$ model with a varying fraction $0.0 \leq p \leq 0.5$ of antiferromagnetic bonds. In principle, the GS for this model is highly degenerate [36]. Here, we investigate only one randomly obtained GS for each realization of the disorder. From a FSS analysis for systems of size $L = 32, 48, 64, 96$, where averages are computed over 3×10^4 samples, we found $p_c = 0.1022(3)$, $\nu_F = 1.47(6)$, $\beta_F = 0.037(4)$ and $\gamma_F = 2.8(1)$. The numerical values of the critical exponents for the $\pm J$ model agree, within errorbars, with those obtained for Model II above. Further, the critical concentration of antiferromagnetic bonds is in fair agreement with the value $p_c = 0.103(1)$ found from an analysis of the Binder parameter within a previous study [31]. Regarding the FSS analysis and compared to [31], we used a larger number of interpolation points that enclose the critical point on the rescaled abscissa (24 data points in the interval $[-0.5 : 0.5]$ for each system size). As a result we obtained p_c with increased precision, although our system sizes are somewhat smaller. Finally, right at p_c we found the critical ratios $\langle M_2/M_1 \rangle = 0.104(1)$ and $\langle M_2 \rangle / \langle M_1 \rangle = 0.083(1)$. The numerical values of these ratios differ slightly from those obtained for Model II above. However, in both cases we observe $\langle M_2/M_1 \rangle \approx 0.125 \langle M_2 \rangle / \langle M_1 \rangle$.

As mentioned above, the scaling of the size ratio according to equation 6 was also confirmed for usual random percolation [35]. It stems from the fact that the largest and second-largest clusters exhibit the same fractal dimension at the critical point. For usual percolation this was shown earlier [37]. While we could verify equation (6) for the disorder induced SG to FM transition at $T = 0$ numerically, we found within additional simulations no such scaling behavior for the thermal phase transition in the 2d Ising ferromagnet.

IV. SUMMARY

We have investigated MEDWs for two-dimensional random-bond Ising spin systems, regarding two different continuous bond distributions. For both models, a disorder parameter could be used to distinguish between a spin-glass ordered or a ferromagnetic ground state. We performed a FSS analysis to locate the critical points in both models that separate the spin-glass phase from the ferromagnetic phase. We found that within the spin-glass phase, the exponents that describe the size scaling of the width of the average DW energy and the average DW length are approximately constant and consistent with the SLE scaling relation previously proposed for the pure spin-glass. Right at the critical point and in the ferromagnetic phase of the models the accordant exponents are not in agreement with the SLE scaling relation.

It is intriguing to note that the fractal dimension of the DWs at the critical point of both disorder types studied here, agrees with the fractal dimension $d_{\text{opt}} = 1.22(2)$ of optimal paths in the strong disorder limit on $2d$ lattices [38]. This is quite interesting since the optimization criteria of the two problems are rather distinct: In the strong disorder limit, nonnegative edge weights are drawn from a very broad distribution. The cost of a path between two sites on the lattice is then dominated by the largest edge-weight along the path. Consequently, so as to find an optimal path, one has to minimize the largest weight along the path. In contrast to this, the cost of a MEDW is the sum of all edge weights along the respective

lattice path. There are positive and also negative edge weights that can cancel each other, at least partially. A common feature of the above two problems is that, in striking contrast to usual shortest path problems, there is no immediate negative feedback for the inclusion of additional path segments. In usual shortest path problems, where there are only positive edge weights, like e.g. optimal paths subject to weak disorder [33], the inclusion of additional path segments leads very likely to an increased path weight. Hence, positive-weight minimum-weight paths tend to be short, which results in an average end-to-end distance $\sim L$.

Finally, we have characterized the SG to FM transition at $T=0$ in terms of the largest and second-largest ferromagnetic clusters of spins found for the GS spin configurations. The respective critical exponents support our previous results and they appear to be consistent with a hyperscaling relation known from scaling theory.

Acknowledgments

We acknowledge financial support from the VolkswagenStiftung (Germany) within the program “Nachwuchsgruppen an Universitäten”. The simulations were performed at the workstation cluster of the “Institute for Theoretical Physics” in Göttingen (Germany) and the GOLEM I cluster for scientific computing at the University of Oldenburg (Germany).

-
- [1] K. Binder and A. Young, Rev. Mod. Phys. **58**, 801 (1986).
 - [2] K. Fischer and J. Hertz, *Spin Glasses* (Cambridge University Press, Cambridge, 1991).
 - [3] M. Mézard, G. Parisi, and M. Virasoro, *Spin glass theory and beyond* (World Scientific, Singapore, 1987).
 - [4] A. P. Young, ed., *Spin glasses and random fields* (World Scientific, Singapore, 1998).
 - [5] W. L. McMillan, J. Phys. C: Solid State Physics **17**, 3179 (1984).
 - [6] D. S. Fisher and D. A. Huse, Phys. Rev. Lett. **56**, 1601 (1986).
 - [7] D. S. Fisher and D. A. Huse, Phys. Rev. B **38**, 386 (1988).
 - [8] A. K. Hartmann, in *Rugged Free Energy Landscapes*, edited by J. W (Springer, Berlin, 2007), pp. 67 – 106.
 - [9] A. K. Hartmann and H. Rieger, *Optimization Algorithms in Physics* (Wiley-VCH, Weinheim, 2001).
 - [10] I. Bieche, R. Maynard, R. Rammal, and J. P. Uhry, J. Phys. A: Math. Gen. **13**, 2553 (1980).
 - [11] F. Barahona, J. Phys. A: Math. Gen. **15**, 3241 (1982).
 - [12] G. Pardella and F. Liers, Phys. Rev. E **78**, 056705 (2008).
 - [13] A. K. Hartmann and A. P. Young, Phys. Rev. B **64**, 180404 (2001).
 - [14] A. K. Hartmann, A. J. Bray, A. C. Carter, M. A. Moore, and A. P. Young, Phys. Rev. B **66**, 224401 (2002).
 - [15] O. Melchert and A. K. Hartmann, Phys. Rev. B **76**, 174411 (2007).
 - [16] C. Amoruso, E. Marinari, O. C. Martin, and A. Pagnani, Phys. Rev. Lett. **91**, 087201 (2003).
 - [17] A. K. Hartmann and A. P. Young, Phys. Rev. B **66**, 094419 (2002).
 - [18] A. K. Hartmann and M. A. Moore, Phys. Rev. Lett. **90**, 127201 (2003).
 - [19] A. K. Hartmann and M. A. Moore, Phys. Rev. B **69**, 104409 (2004).
 - [20] A. K. Hartmann, Phys. Rev. B **77**, 144418 (pages 5) (2008).
 - [21] C. Amoruso, A. K. Hartmann, M. B. Hastings, and M. A. Moore, Phys. Rev. Lett. **97**, 267202 (pages 4) (2006).
 - [22] D. Bernard, P. Le Doussal, and A. A. Middleton, Phys. Rev. B **76**, 020403 (pages 4) (2007).
 - [23] J. Cardy, Annals of Physics **318**, 81 (2005).
 - [24] F. Krzakala and O. C. Martin, Phys. Rev. Lett. **89**, 267202 (2002).
 - [25] W. L. McMillan, Phys. Rev. B **29**, 4026 (1984).
 - [26] R. K. Ahuja, T. L. Magnanti, and J. B. Orlin, *Network Flows: Theory, Algorithms, and Applications* (Prentice Hall, 1993).
 - [27] M. E. J. Newman and R. M. Ziff, Phys. Rev. Lett. **85**, 4104 (2000).
 - [28] K. Binder, Z. Phys. B **43**, 119 (1981).
 - [29] J. Houdayer and A. K. Hartmann, Phys. Rev. B **70**, 014418 (2004), S measures the mean square distance of

the scaled data to the master curve in units of standard errors.

- [30] O. Melchert and A. K. Hartmann, New. J. Phys. **10**, 043039 (2008).
- [31] C. Amoruso and A. K. Hartmann, Phys. Rev. B **70**, 134425 (2004), Note that the value of $\beta = 0.9(1)$ is a misprint and should read $\beta = 0.09(1)$.
- [32] D. A. Huse and C. L. Henley, Phys. Rev. Lett. **54**, 2708 (1985).
- [33] N. Schwartz, A. L. Nazaryev, and S. Havlin, Phys. Rev. E **58**, 7642 (1998).
- [34] M. Kardar and Y. C. Zhang, Phys. Rev. Lett. **58**, 2087 (1987).
- [35] C. R. da Silva, M. L. Lyra, and G. M. Viswanathan, Phys. Rev. E **66**, 056107 (2002).
- [36] J. W. Landry and S. N. Coppersmith, Phys. Rev. B **65**, 134404 (2002).
- [37] N. Jan, D. Stauffer, and A. Aharony, J. Stat. Phys. **92**, 325 (1998).
- [38] M. Cieplak, A. Maritan, and J. R. Banavar, Phys. Rev. Lett. **72**, 2320 (1994).